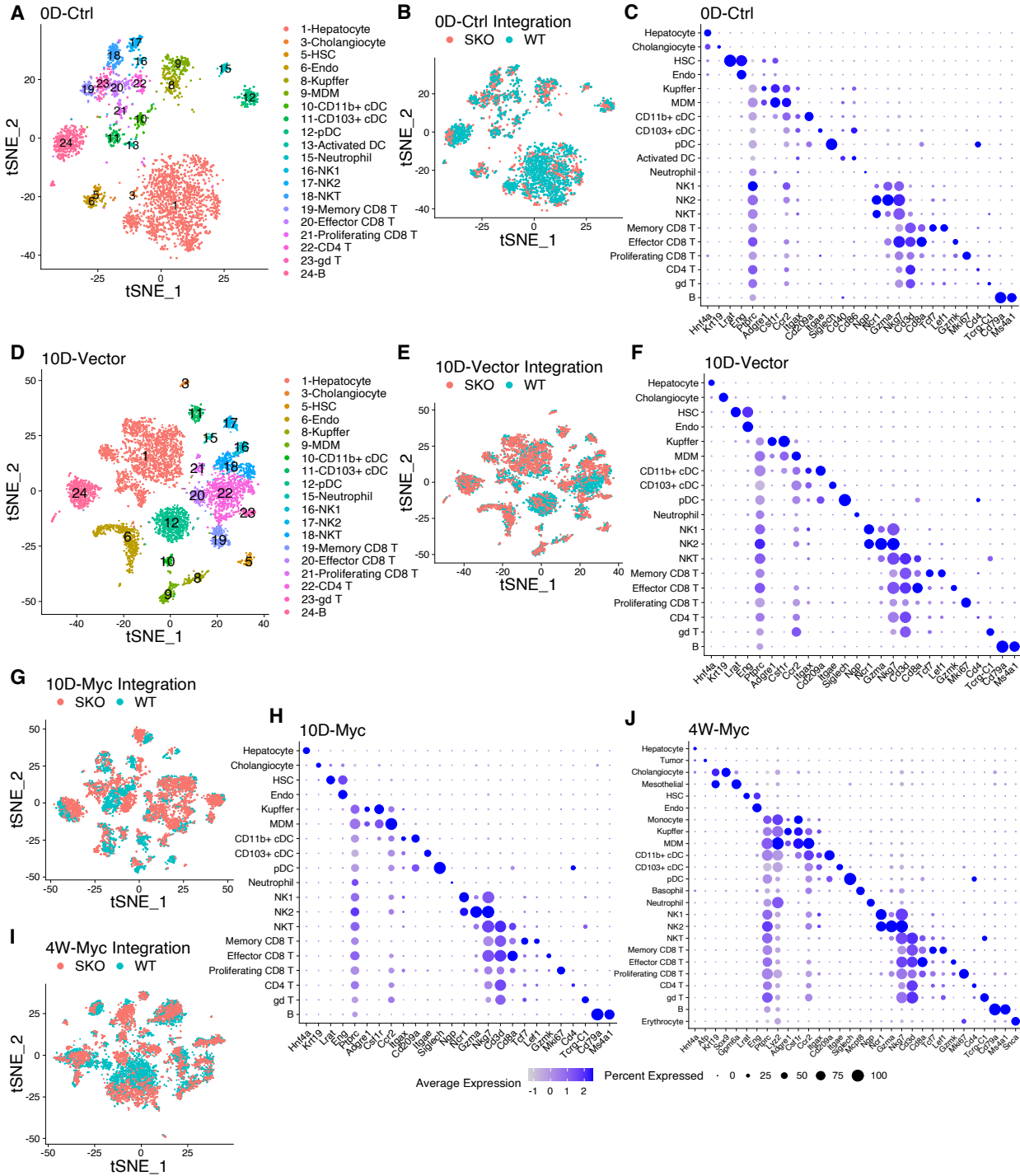


**Cell Reports, Volume 37**

**Supplemental information**

**Single-cell transcriptomics reveals  
opposing roles of Shp2 in Myc-driven  
liver tumor cells and microenvironment**

**Wendy S. Chen, Yan Liang, Min Zong, Jacey J. Liu, Kota Kaneko, Kaisa L. Hanley, Kun Zhang, and Gen-Sheng Feng**



**Figure S1. Additional quality control plots associated with scRNA-seq data integration, Related to Figure 2.**

(A) tSNE plot showing clusters of single cells from WT and SKO livers at 0D (before HTVi procedure). Colored dots label cell types identified in each cluster.

(B) Integrated tSNE plots of 0D-Ctrl differentiating data used in integrated t-clustering where red and blue dots indicate SKO and WT livers, respectively.

(C) Important marker genes used for cell type assignment in 0D-Ctrl data and their expression levels in said cell type clusters.

(D) tSNE plot showing clusters of single cells from WT and SKO livers 10 days post-HTVi of empty vector. Colored dots label cell types identified in each cluster.

(E) Integrated tSNE plot of 10D-Vector differentiating data used in integrated t-clustering where red and blue dots indicate SKO and WT livers, respectively.

(F) Important marker genes used for cell type assignment in 10D-Vector data and their expression levels in said cell type clusters.

(G) Integrated tSNE plot relative to Figure 2B (10D-Myc data), where red and blue dots are SKO and WT, respectively.

(H) Important marker genes used for cell type assignment in 10D-Myc data and their expression levels in said cell type clusters.

(I) Integrated tSNE relative to Figure 2C (4W-Myc data) differentiating data used in integrated t-clustering where red and blue dots are SKO and WT, respectively.

(J) Marker genes used for cell type assignment in 4W-Myc integrated data and their expression levels in said cell type clusters.

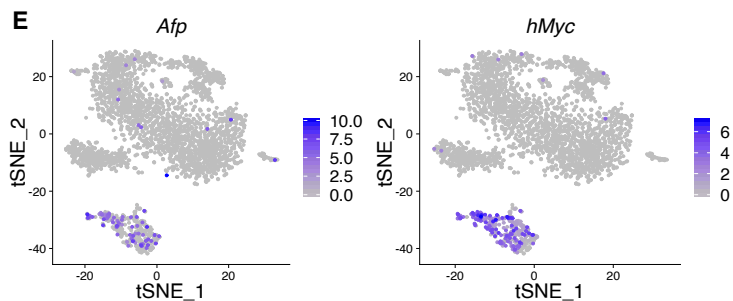
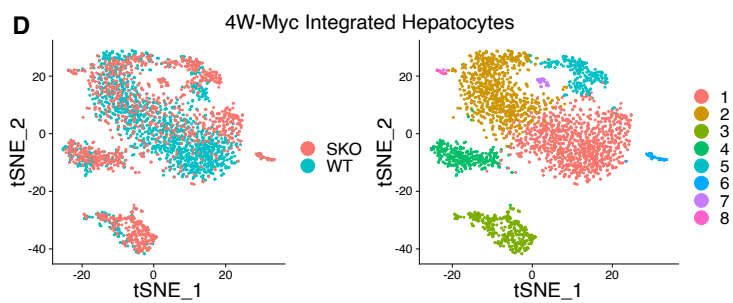
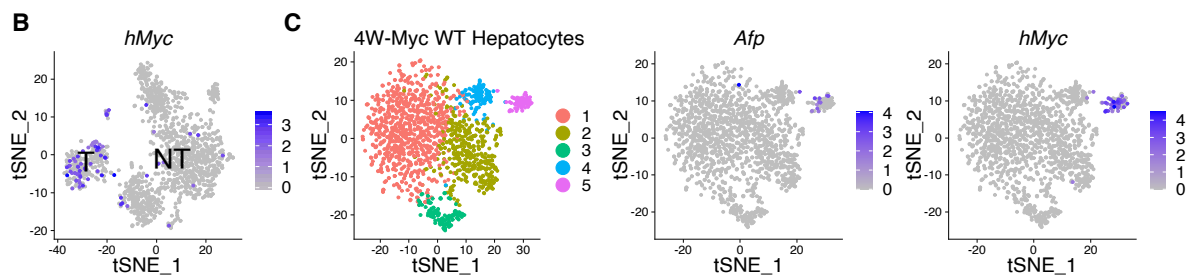
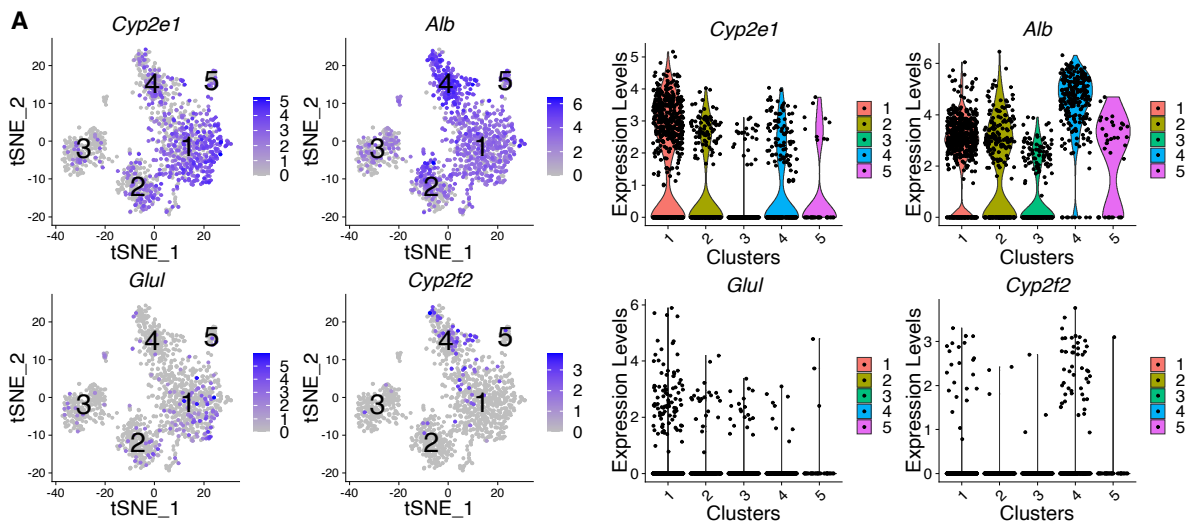


**Figure S2. Analysis of 4W-Myc scRNA-seq data on hepatocytes and tumor populations, Related to Figure 2.**

**(A)** 4W-Myc SKO hepatocyte clusters showing tSNE plot (left) and violin plot (right) for expression profiles of known liver zonation markers Cyp2e1, Albumin (Alb), Glutamine synthetase (Glul), and Cyp2f2 in hepatocyte clusters.

**(B)** tSNE plot of data from Figure 2D (4W-Myc SKO hepatocyte) where blue dots show higher expression of Myc (exogenous Myc) in tumor than non-tumor cells.

**(C)** tSNE plot of hepatocyte clustering from 4W-Myc WT liver showing hepatocyte clustering (left) and expression profiles of AFP and Myc (right). Clusters include: (1) peri-portal hepatocytes; (2) mid-zone hepatocytes; (3) peri-central vein hepatocytes; (4) OxPhos & translation-related hepatocytes; (5) Tumor cells.

**(D)** tSNE plot of integrated 4W-Myc hepatocyte data where red and blue dots are WT and SKO (left), and various colors define hepatocyte clustering (right). Clusters include: (1) peri-portal hepatocytes; (2) mid-zone hepatocytes; (3) Tumor cells; (4) OxPhos & translation-related hepatocytes; (5) peri-central hepatocytes; (6) Malat1hi hepatocytes; (7) Usp31+ hepatocytes; (8) Cd24a+ hepatocytes.

**(E)** AFP and Myc expression profile on tSNE plot of integrated WT and SKO 4W-Myc hepatocyte data showing Afp+ (left) and Myc+ (right) hepatocytes as blue dots. Myc+ hepatocytes from WT and SKO cluster together, indicating Myc+ populations are tumor cells in both of them.

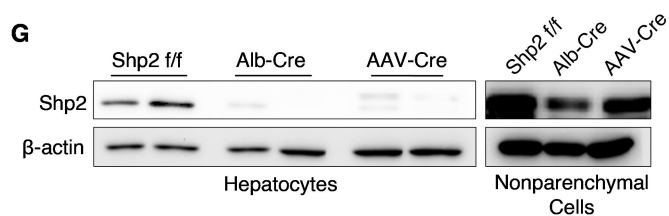
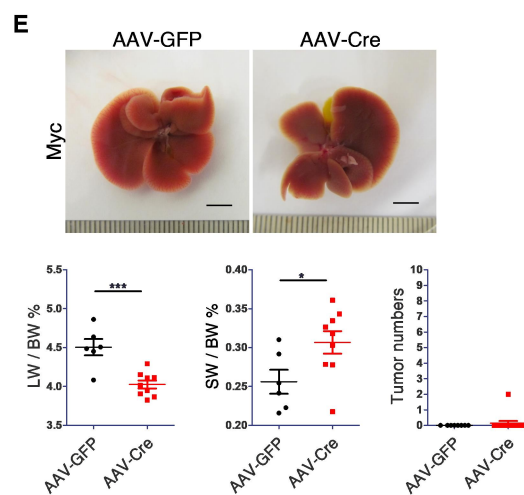
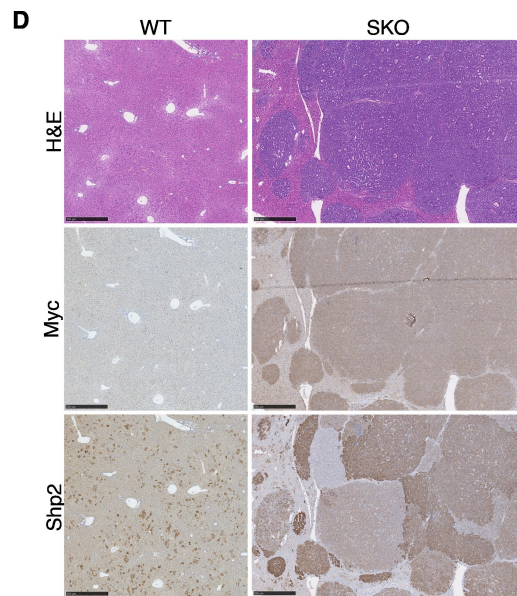
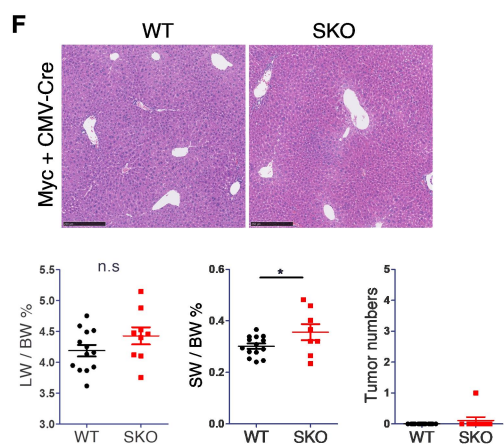
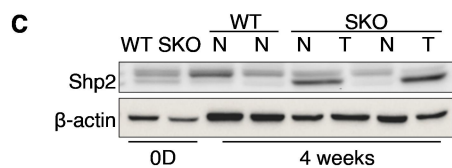
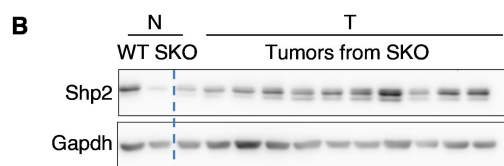
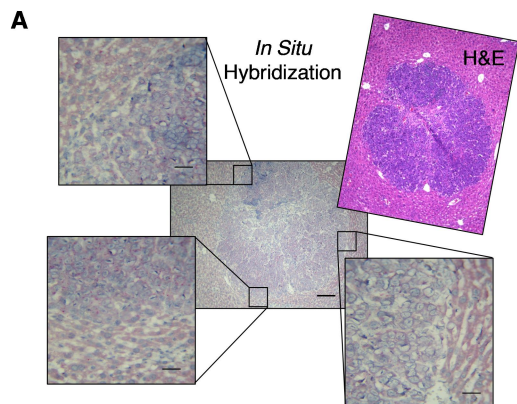


**Figure S3. Shp2 presence in Myc+ tumors in SKO livers, Related to Figure 3.**

(A) In situ hybridization of Shp2 detecting *Ptpn11/Shp2* mRNA in tumors at 4 weeks post-Myc injection. In pathological comparison to H&E staining in consecutive sections, Shp2 mRNA levels were high in tumor areas. Scale bar, 50  $\mu$ m.

(B) Immunoblotting of liver lysates from non-tumor (N) and tumor (T) tissues 4 weeks after Myc transfection indicating variable but increased Shp2 expression in tumor tissues.

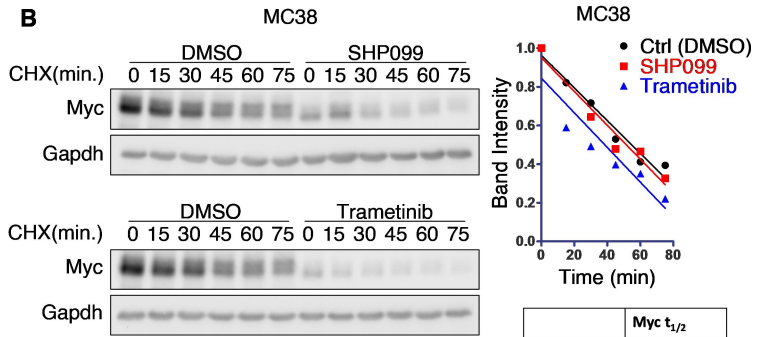
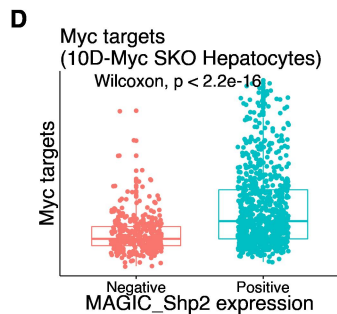
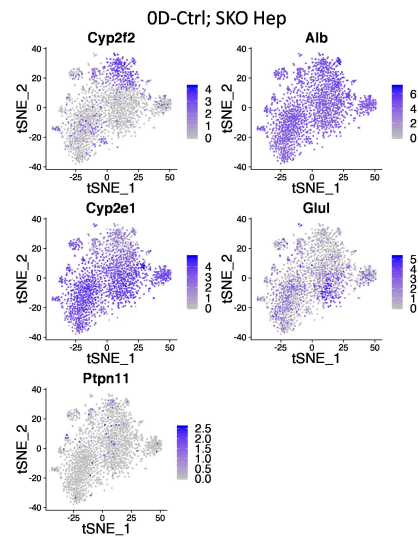
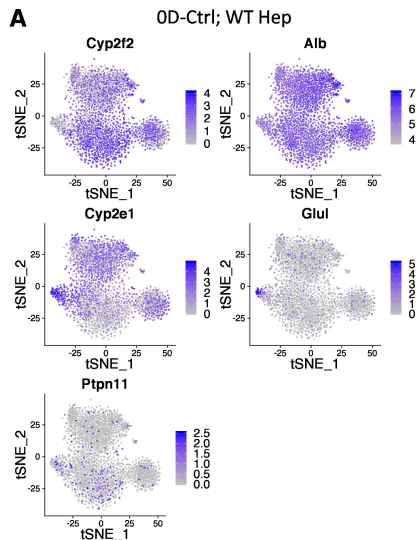
(C) Immunoblotting of isolated hepatocyte lysates from WT and SKO livers at 0 day and 4 weeks after HTVi of Myc.

(D) Representative H&E, and immunostaining for Myc and Shp2 in consecutive sections of SKO livers 3 weeks after transfection by Myc+Shp2. Scale bar, 500  $\mu$ m.

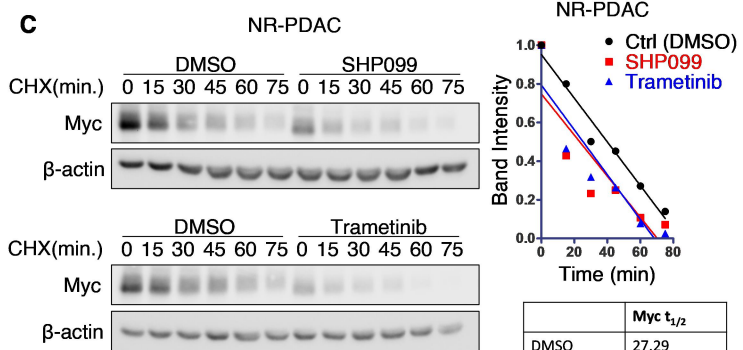
(E) WT (*Shp2<sup>f/f</sup>*) mice were injected with AAV-GFP (n=6) or AAV-Cre (n=9) virus 1 wk before Myc transfection via HTVi, and examined at 4wk after Myc transfection. Representative liver images (left) and liver to body weight ratios (right). Scale bar, 0.5 cm. Quantification of LW/BW, SW/BW, and tumor numbers of mice at 4 weeks. Students T-test: (\*  $p < 0.05$ , \*\*\*  $p$ -value  $< 0.001$ ).

(F) Representative H&E staining showing lack of tumor nodules, of mice 4 weeks post-HTVi of Myc + CMV-Cre with quantification of LW/BW, SW/BW, and tumor numbers. Scale bar, 250  $\mu$ m. Students T-test (\*  $p < 0.05$ ).

(G) Shp2 protein level in hepatocyte and non-parenchymal cell lysate from WT *Shp2<sup>f/f</sup>*, Albumin-cre, and AAV-Cre hepatocyte knock-out murine models at 8 weeks of age.



	Myc $t_{1/2}$
DMSO	54.49
SHP099	51.19
Trametinib	38.29



	Myc $t_{1/2}$
DMSO	27.29
SHP099	23.34
Trametinib	25.28

**E**

Pathways positively regulated in Shp2- Myc+ (vs Shp2- Myc-)	FDR $q$ value
REACTOME_THE_CITRIC_ACID_TCA_CYCLE_AND_RESPIRATORY_ELECTRON_TRANSPORT	2.48E-17
REACTOME_RESPIRATORY_ELECTRON_TRANSPORT_ATP_SYNTHESIS_BY_CHEMIOSMOTIC_COUPLING_AND_HEAT_PRODUCTION_BY_UNCOUPLING_PROTEINS	1.79E-16
HALLMARK_OXIDATIVE_PHOSPHORYLATION	2.96E-15
REACTOME_RESPIRATORY_ELECTRON_TRANSPORT_WP_ELECTRON_TRANSPORT_CHAIN_OXPPOS_SYSTEM_IN_MITOCHONDRIA	3.12E-14
KEGG_PARKINSONS_DISEASE	1.47E-11
KEGG_OXIDATIVE_PHOSPHORYLATION	5.97E-10
WP_NONALCOHOLIC_FATTY_LIVER_DISEASE	3.60E-09
REACTOME_TRANSLATION	3.88E-09

**Figure S4. Shp2+ hepatocytes function, Related to Figure 3.**

(A) scRNA-seq analysis showing expression of zonation markers and Ptpn11 at 0D-Ctrl timepoint in WT and SKO hepatocyte data.

(B-C) Immunoblot and quantification of Myc protein expression and half-life, in MC38 (B) and NR-PDAC (C) cell lysates collected at indicated time points following treatment with CHX (MC38 cells: 50  $\mu\text{g}/\text{mL}$ ; NR-PDAC cells: 25  $\mu\text{g}/\text{mL}$ ), after pre-treatment with SHP099 (Shp2 inhibitor; 20  $\mu\text{M}$ ) for 16 hr or Trametinib (Mek inhibitor; 50  $\mu\text{M}$ ) for 4 hr, with DMSO as control. Related to Figure 3D

(D) Box plot of 10D-Myc SKO data demonstrating hepatocytes with correlated expression levels of MAGIC-imputed Shp2 and Myc target genes.

(E) Unsupervised pathway enrichment analysis identified top results of Shp2-Myc+ cells, as compared to Shp2-Myc- cells, in SKO liver indicating pathways upregulated in Myc+ tumor cells.

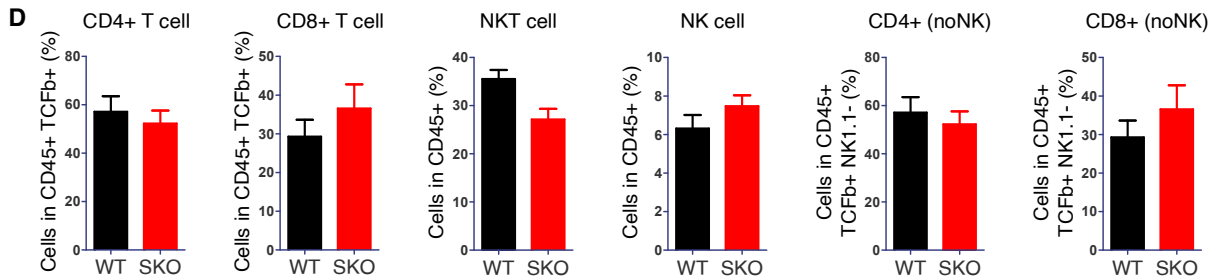
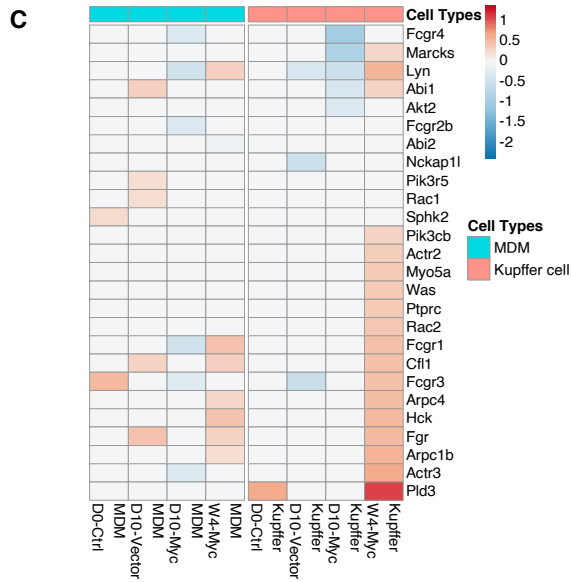
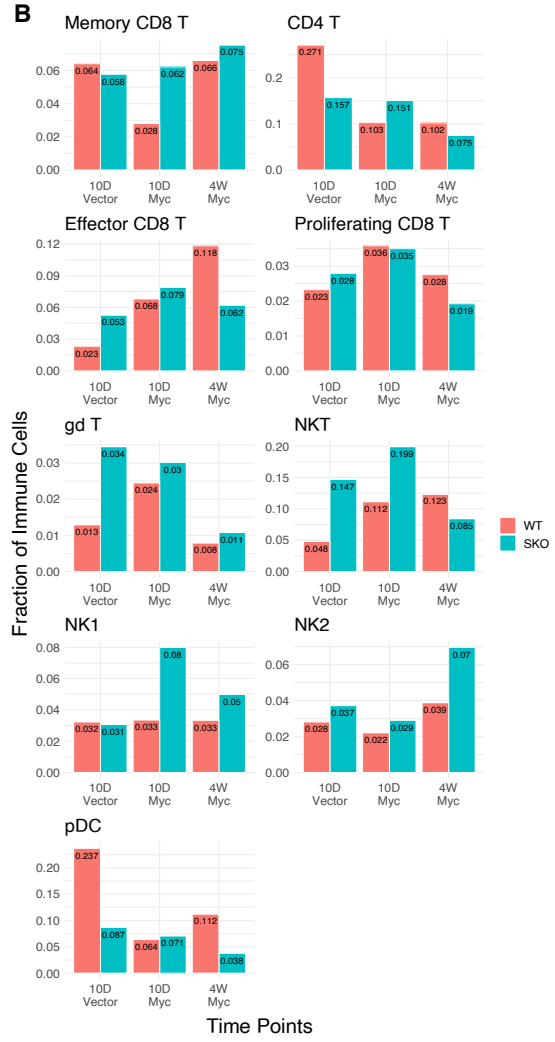
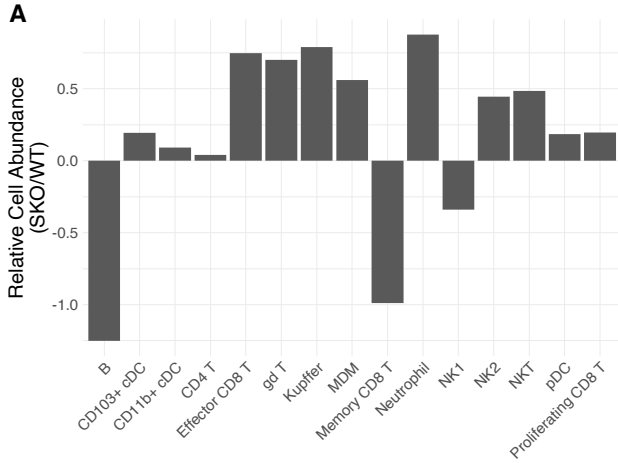


**Figure S5. Characterization of immune cell populations by scRNA-seq analysis and FACS, Related to Figure 4 and 5.**

(A) Comparison of quantified immune cell populations between SKO and WT liver, based on 0D-Ctrl data. For each cell type, the relative cell abundance was calculated as the log-transformed ratios of SKO vs WT percentages.

(B) Quantified cell populations of WT and SKO livers between 10D-Vector, 10D-Myc, and 4W-Myc: naïve CD8 T, CD4 T, effector T, proliferating CD8 T, DN T, NKT, NK1, NK2, and pDC cell populations. Additional populations are depicted in Figure 4B.

(C) Differential expression analysis of phagocytosis genes for MDMs (Blue) and Kupffer cells (Red) at all time points. The values in the heatmap indicate averaged log<sub>2</sub> fold changes in SKO over WT livers, for corresponding cell types at different time points. As related to Figure 4D.

(D) FACS of immune cell populations 12 days post-Myc injection in isolated non-parenchymal cells: CD45<sup>+</sup> and TCRβ<sup>+</sup> gated CD4<sup>+</sup> and CD8<sup>+</sup> T cells (Left); CD45<sup>+</sup> NKT (NK1.1<sup>+</sup> TCRβ<sup>+</sup>) and NK (NK1.1<sup>+</sup> TCRβ<sup>-</sup>) cells (Middle); and CD45<sup>+</sup> TCFβ<sup>+</sup> NK1.1<sup>-</sup> gated CD4<sup>+</sup> and CD8<sup>+</sup> T cells (Right). No significant difference in these cell types was observed between WT and SKO mice. Values are presented as means ± SD. (ns,  $p > 0.05$ , student's T-test).

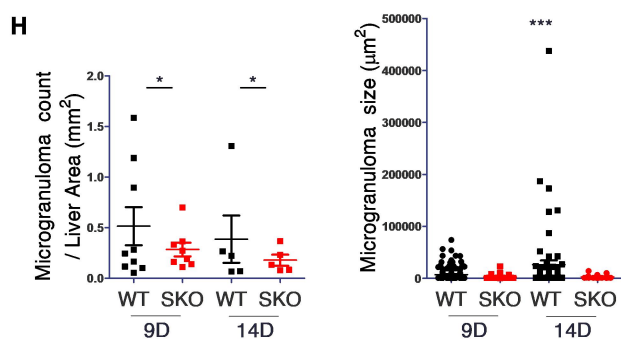
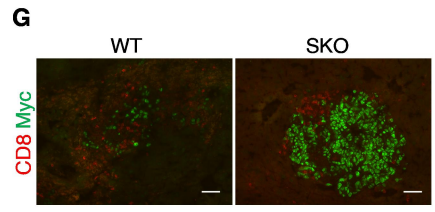
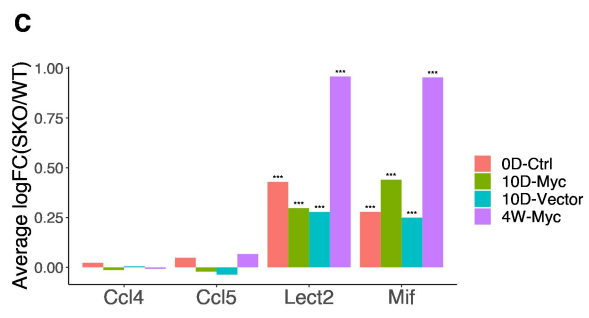
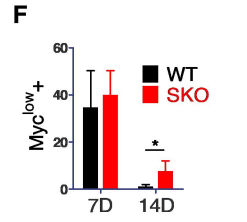
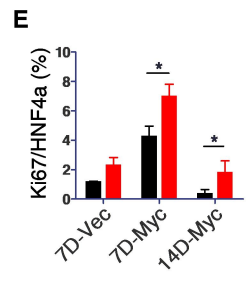
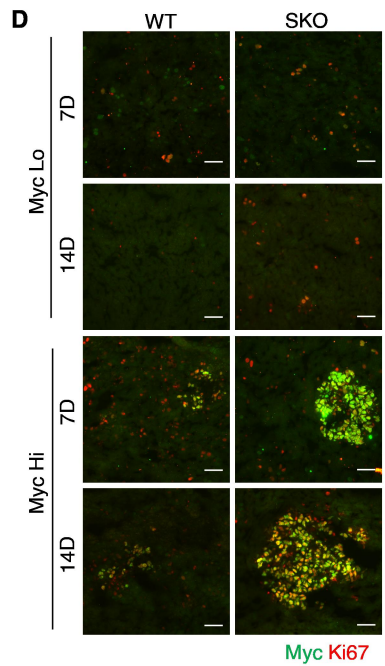
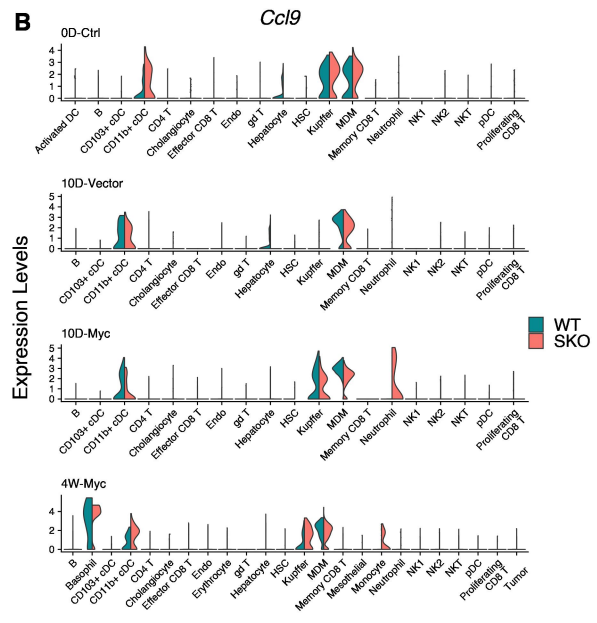
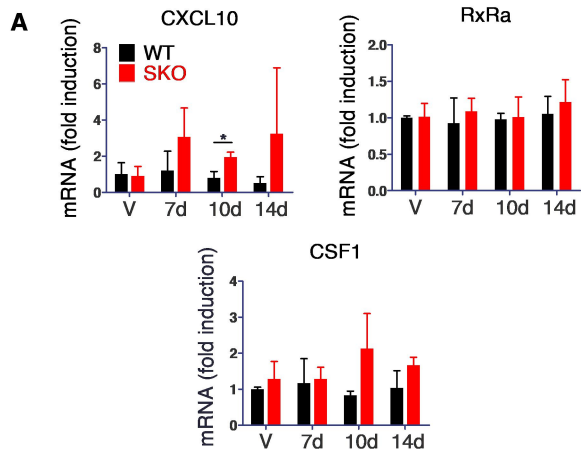


**Figure S6. Further characterization of the immune microenvironment of Myc-induced tumors, Related to Figure 5.**

(A) qRT-PCR analysis CXCL10, RxR $\alpha$  and CSF1 expression in WT and SKO liver lysates 7D after vector injection, and 7D, 10D, 14D after Myc injection.

(B) Violin plots comparing Ccl9 expression between WT and SKO in each cell type as indicated, in 0D-Ctrl, 10D-Vector, 10D-Myc, and 4W-Myc data.

(C) Bar plots comparing indicated ligands expression between WT and SKO hepatocytes at each time point. Values are presented as log fold-change of the average expression. Positive values indicate higher expression in SKO hepatocytes.

(D) Staining of Myc and Ki67 in WT and SKO livers 7 and 14 days post Myc injection, in Myc<sup>Lo</sup> and Myc<sup>Hi</sup> cell colonies. Scale bar, 50  $\mu$ m.

(E-F) Quantified cell numbers of Ki67+ per HNF4 $\alpha$ + (E), Ki67+ per Myc<sup>Lo</sup> (F) in WT and SKO livers at 7D and 14D after HTVi.

(G) Co-staining of Myc with CD8 in WT and SKO livers at 10d post-HTVi of Myc. Scale bar, 100  $\mu$ m.

(H) Quantified microgranuloma area per tissue area in WT and SKO liver at 9D and 14D.

Statistical analysis used student's T-test. (\* p < 0.05, \*\*\* p-value < 0.001).

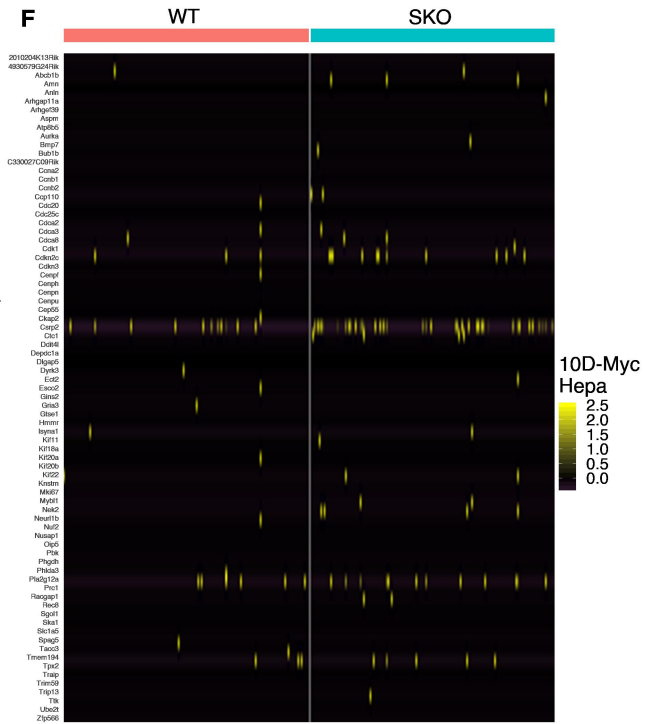
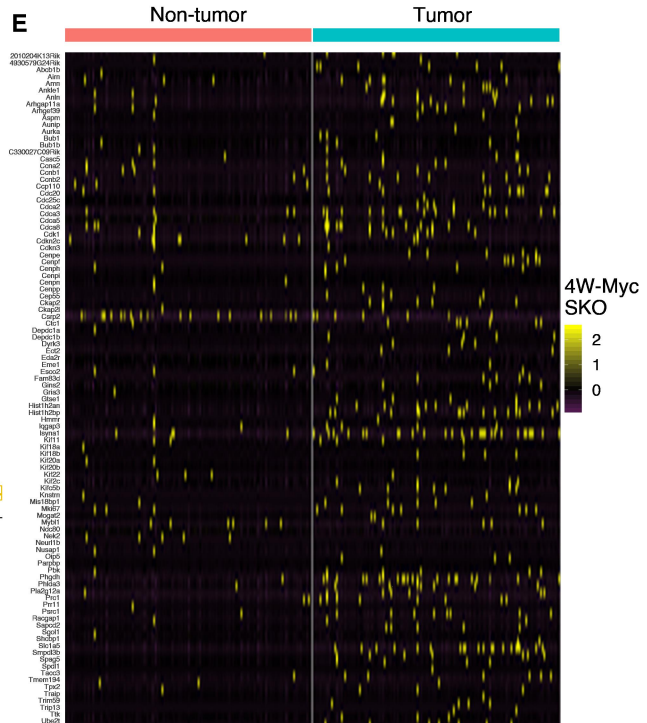
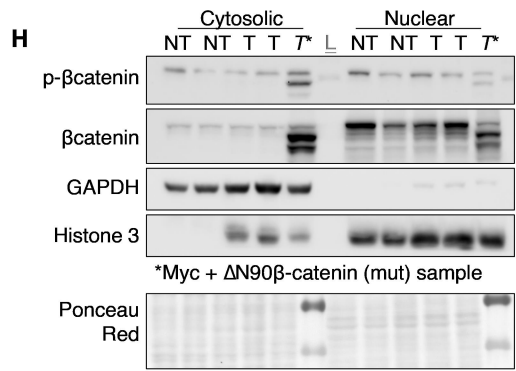
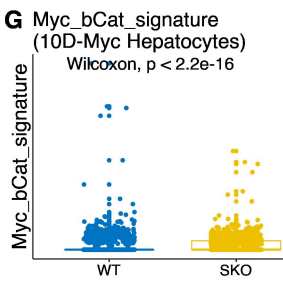
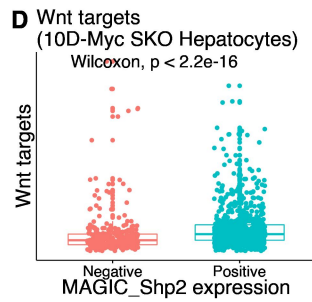
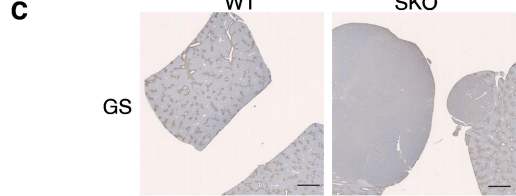
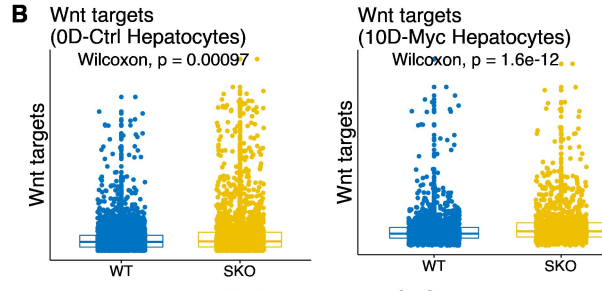
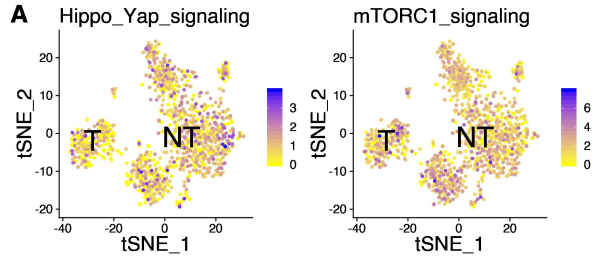


**Figure S7. scRNA-seq detects upregulation of basal and Myc-induced  $\beta$ -catenin signaling, Related to Figure 6.**

(A) tSNE plot of scores defined for Hippo/YAP and mTORC1 pathway genes in 4W-Myc SKO data, showing no significant change in pathway expression in tumor vs non-tumor cells.

(B) Boxplots comparing scores defined for Wnt target genes at 0D-Ctrl (Left) and 10D-Myc (Right) time points. Wnt target gene levels were modestly higher in SKO than WT. Related to Figure 6B.

(C) Low magnification view of immunohistochemistry staining of Glutamine Synthetase (GS) from Figure 6C. Scale bar, 1 cm.

(D) Box plot of 10D-Myc SKO hepatocytes. Cells with positive Shp2 expression had higher expression of Wnt target genes.

(E-F) Heatmap showing expression profile of genes in “Myc/ $\beta$ -catenin signature” (Bisso *et al.*, 2020), between tumor and non-tumor hepatocytes in 4W-Myc data in SKO liver (E) related to Figure 6B, and WT and SKO in 10D-Myc data (F) related to Figure S7G. Each column is a single cell, each row is a gene.

(G) Boxplot showing scores defined for the “Myc/ $\beta$ -catenin signature” in 10D-Myc hepatocytes, relative to 4W-Myc data in Figure 6D.

(H) Immunoblot of tumor (T) and non-tumor (NT) lysates 4 weeks after transfection of Myc or Myc+ $\Delta$ N90- $\beta$ -catenin tumor lysate (T\*), separated by protein ladder (L) between cytosolic and nuclear fractions, with Ponceau red showing loading controls.

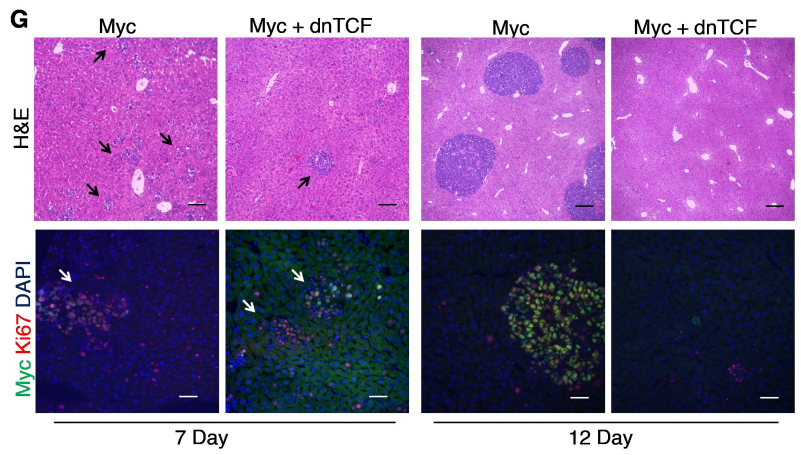
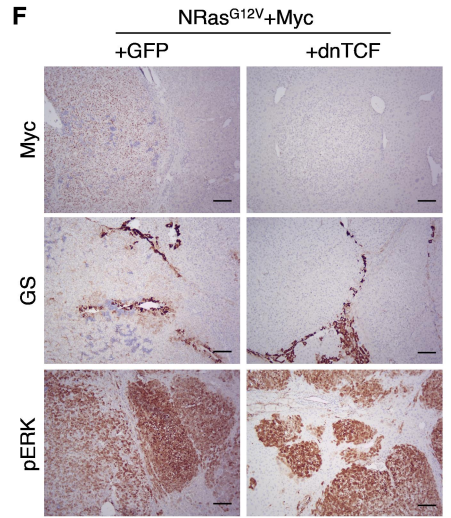
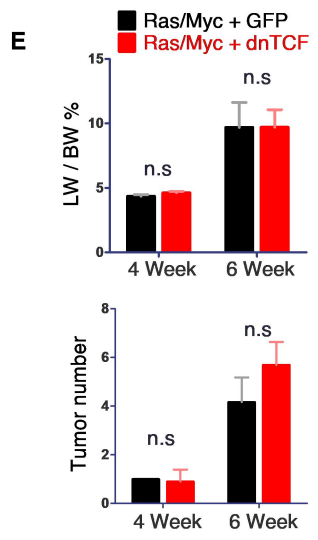
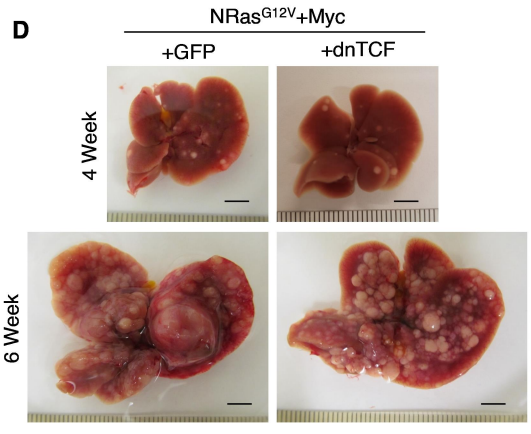
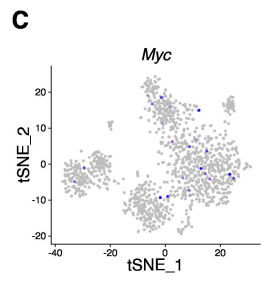
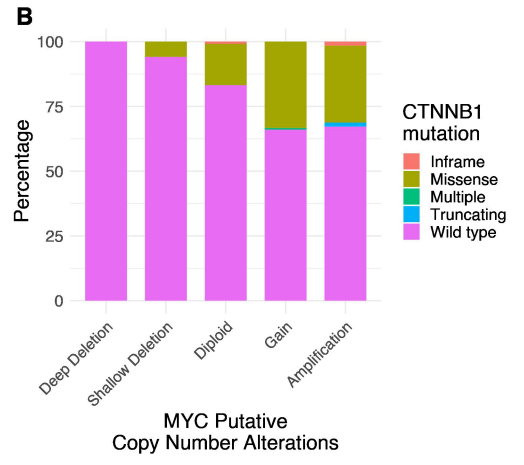
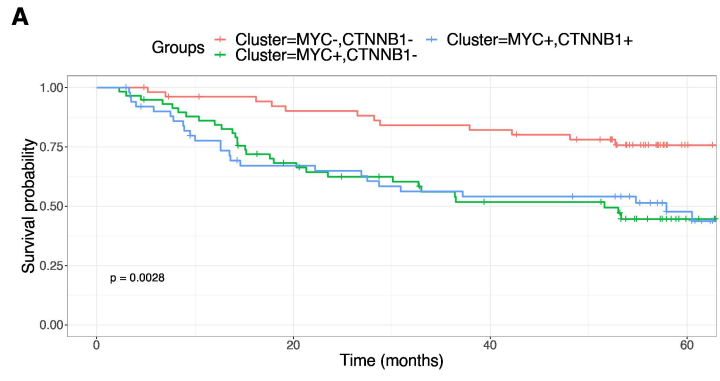


**Figure S8. Transcriptional repression of  $\beta$ -catenin does not affect Ras/Myc tumor growth, Related to Figure 7.**

(A) Kaplan-Meier survival analysis of patients from GSE14520 dataset with MYC<sup>-</sup> CTNNB1<sup>-</sup>, MYC<sup>+</sup> CTNNB1<sup>-</sup>, and MYC<sup>+</sup> CTNNB1<sup>+</sup> based on mRNA expression levels. The MYC<sup>+</sup> CTNNB1<sup>+</sup> Patients exhibited significantly worse survival.

(B) HCC patients' data in TCGA were separated by MYC copy number alterations into columns and then distinguished by CTNNB1 mutation profiles within each column. Patients with higher MYC copy number alterations have increased CTNNB1 mutation loads.

(C) tSNE plot of endogenous Myc levels in 4W-Myc SKO hepatocyte data, showing lack of correlation between hepatocyte cluster and Myc expression.

(D) Representative images of WT livers at 4 and 6 weeks post-HTVi of NRas<sup>G12V</sup> (Ras)/Myc + GFP or Ras/Myc + dnTCF. (4 week, n=4; 6 week, n=10). Scale bar, 0.5 cm.

(E) Quantification of liver to body weight ratios (LW/BW) and tumor numbers of livers from S9A. Statistical significance calculated by students T-test. Values are presented as means  $\pm$  SD. (n.s. P>0.05).

(F) Representative staining for Myc, GS, and p-Erk in WT livers 6 weeks after HTVi of Ras/Myc + GFP or Ras/Myc + dnTCF. Scale bar, 250  $\mu$ m.

(G) Representative H&E (top) and immunostaining of Myc and Ki67 (bottom) in SKO livers 7 and 12 days after HTVi of Myc or Myc + dnTCF. Top Scale bar, 250  $\mu$ m. Bottom Scale bar, 100  $\mu$ m.

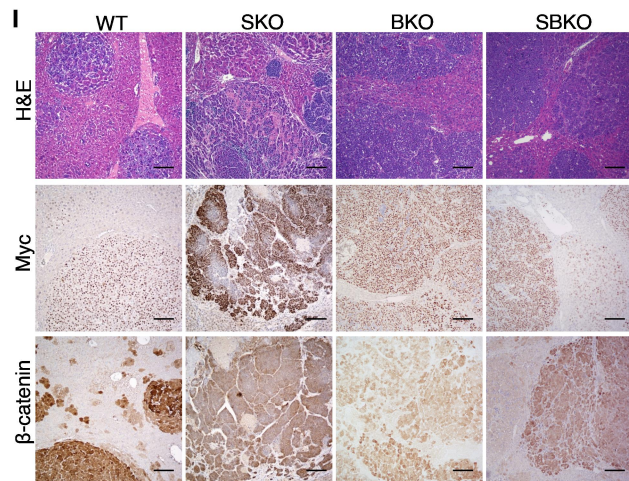
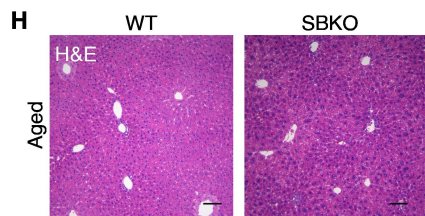
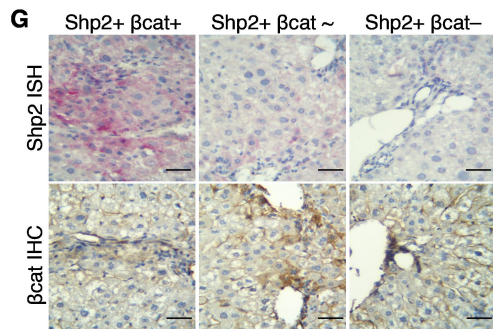
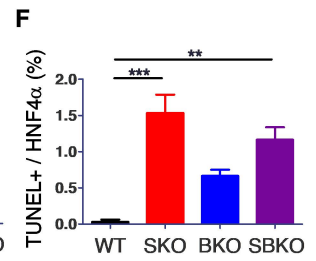
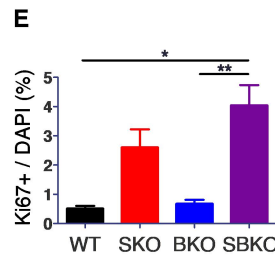
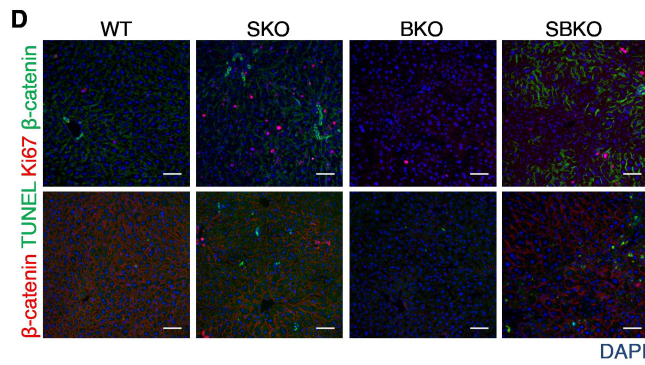
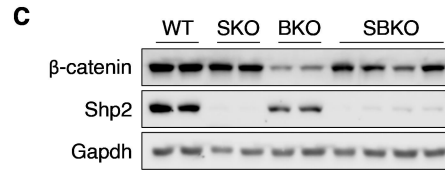
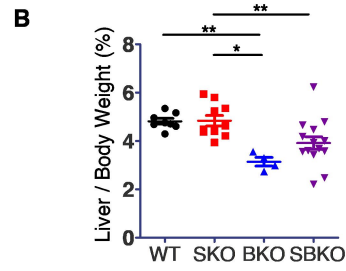
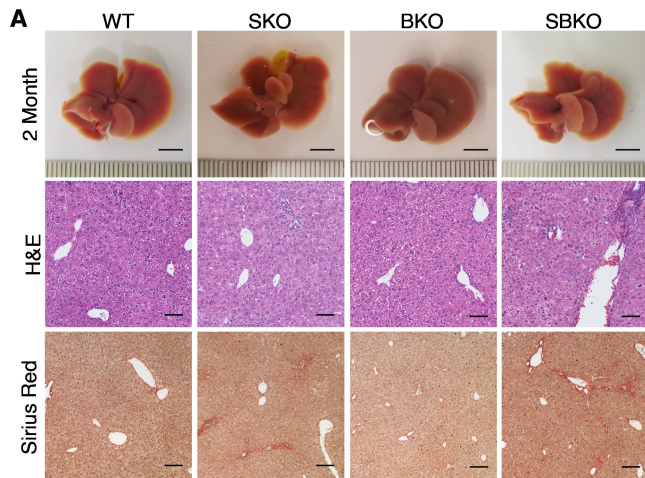


**Figure S9. Characterization of SBKO liver deficient for Shp2 and  $\beta$ -catenin, Related to Figure 7.**

(A) Representative images of WT, SKO, BKO, and SBKO livers at 2 months, with Liver (top), H&E (middle), and Sirius red staining (bottom). Liver scale bar, 0.5 mm. Staining scale bar, 250  $\mu$ m.

(B) Quantification of liver to body weight ratios, (n=10).

(C) Immunoblot showing Shp2 and  $\beta$ -catenin deletion in respective genotypes.

D-F) Representative immunostaining of Ki67 and  $\beta$ -catenin (top) and  $\beta$ -catenin and TUNEL (bottom) in respective genotypes, with quantification of Ki67+/DAPI (E) and TUNEL+/HNF4 $\alpha$  (F). n=5, Scale bar, 100  $\mu$ m.

(G). In situ hybridization of Shp2 and immunostaining of  $\beta$ -catenin in consecutive sections. Scale bar, 50  $\mu$ m.

(H) H&E staining showing hepatic architecture of 15-month SBKO livers. Scale bar, 250  $\mu$ m.

Statistical significance calculated by one-sided ANOVA with post-hoc Tukey test. Values are presented as means  $\pm$  SD. (\* p<0.05; \*\* p<0.01; \*\*\* p<0.001).

(I) Representative H&E (Up), immunostaining for Myc (middle) and  $\beta$ -catenin (low) of livers 4 weeks after transfection of Myc and  $\beta$ -catenin in WT, SKO, BKO, and SBKO mice. Scale bar, 250  $\mu$ m.

**Table S1: Tumor Histopathology Analysis, Related to Figure 1, 3, 7.**

Histopathological results of Hematoxylin and Eosin-stained tissue samples of tumor models in SKO mice. Analysis performed by Dr. Nissi Varki (Professor of Pathology, UCSD)

Sample	Genotype	Tumor model	Tumor Histopathology
SJ1268	SKO	Myc	Trabecular HCC, well-differentiated, hepatoblastoma-like features, high nucleus-to-cytoplasmic ratio, highly aggressive, Inflammatory infiltrates
SM707	SKO	Myc	Trabecular HCC, well-differentiated, hepatoblastoma-like features, high nucleus-to-cytoplasmic ratio, highly aggressive
S446	SKO	Myc	Trabecular HCC, well-differentiated, hepatoblastoma-like features, high nucleus-to-cytoplasmic ratio, highly aggressive
S441	SKO	Myc	Trabecular HCC, well-differentiated, hepatoblastoma-like features, high nucleus-to-cytoplasmic ratio, highly aggressive
S425	SKO	Myc	Trabecular HCC, well-differentiated, hepatoblastoma-like features, high nucleus-to-cytoplasmic ratio, highly aggressive
SM705	WT	Myc	Trabecular HCC, well-differentiated, hepatoblastoma-like features, high nucleus-to-cytoplasmic ratio, highly aggressive
S445	WT	Myc	Trabecular HCC, well-differentiated, hepatoblastoma-like features, high nucleus-to-cytoplasmic ratio, highly aggressive
SM30	SKO	Myc + Shp2	Trabecular HCC and highly malignant poorly differentiated HCC, highly aggressive
SM34	SKO	Myc + Shp2	Trabecular HCC and highly malignant poorly-differentiated HCC, highly aggressive
S535-6	SKO	NRas <sup>G12V</sup> + Myc	Well-differentiated HCC, Mallory-Denk bodies
S541	SKO	NRas <sup>G12V</sup> + Myc	Well-differentiated HCC, Mallory-Denk bodies
SB738	SKO	Myc + $\Delta$ N90- $\beta$ -catenin	Hepatoblastoma and well-differentiated HCC
SB739	SKO	Myc + $\Delta$ N90- $\beta$ -catenin	Hepatoblastoma and well-differentiated HCC

**Table S2: Total numbers of cells used for scRNAseq analysis, Related to Figure 2.**

			<b>Before filtering</b>	<b>After filtering</b>	<b>Total after filtering</b>
<b>0D-Ctrl</b>	WT	Hep	1290	1232	4610
		NPC	1600	1100	
	SKO	Hep	1023	871	
		NPC	1930	1407	
<b>10D-Vector</b>	WT	Hep	1290	1195	7888
		NPC	3075	3039	
	SKO	Hep	1297	1293	
		NPC	2497	2361	
<b>10D-Myc</b>	WT	Hep	1000	989	6631
		NPC	1985	1951	
	SKO	Hep	905	886	
		NPC	2888	2805	
<b>4W-Myc</b>	WT	Hep	1349	1349	8198
		NPC	2713	2569	
	SKO	Hep	1381	1373	
		NPC	3024	2907	

**Table S3: Cytokine expression in hepatocytes, Related to Figure 4.**

Ligands expression between WT and SKO hepatocytes at each time point, using scRNA-sequencing. Values are presented as log fold-change of the average expression. Positive values indicate higher expression in SKO hepatocytes

	<b>0D-Ctrl</b>		<b>10D-Vector</b>	
	<b>avg_logFC (SKO/WT)</b>	<b>p_adj</b>	<b>avg_logFC (SKO/WT)</b>	<b>p_adj</b>
Ccl2	0.0228231090	1.00E+00	-0.0348341890	1.00E+00
Ccl4	0.0230392399	1.00E+00	0.0050715960	1.00E+00
Ccl5	0.0484332990	1.00E+00	-0.0364395020	1.00E+00
Ccl6	0.0440357818	1.58E-01	-0.0049858090	1.00E+00
Ccl7	0.0098169779	1.00E+00	Not Detected	
Ccl9	-0.4318557608	1.22E-32	-0.2689959190	3.35E-11
Ccl25	Not Detected		-0.0209034900	1.00E+00
Ccl27a	Not Detected		-0.0073178150	1.00E+00
Cxcl1	-0.1008580890	4.15E-01	-0.4277598090	1.65E-32
Cxcl2	0.0073602910	1.00E+00	Not Detected	
Cxcl9	0.2861360420	6.60E-16	0.0135539410	1.00E+00
Cxcl10	0.0608337100	2.54E-01	0.0167738800	1.00E+00
Cxcl11	0.0064971040	1.00E+00	-0.0314060290	1.00E+00
Cxcl12	-0.0190080910	1.00E+00	-0.0054141520	1.00E+00
Cxcl13	Not Detected		-0.0004689840	1.00E+00
Cxcl14	-0.0045888470	1.00E+00	-0.0179419980	1.00E+00
Cxcl16	0.0437289610	1.00E+00	0.0180524880	1.00E+00
Lect2	0.429395800	6.54E-21	0.2782983000	5.06E-05
Mif	0.278377906	3.34E-05	0.2496263000	7.64E-06
Nampt	0.310062400	8.71E-10	0.0457770400	1.00E+00
Spp1	0.647512450	5.51E-05	0.1547416200	1.00E+00
Vegfa	-0.046265820	1.00E+00	-0.0462658200	1.00E+00

Aimp1	Not Detected		Not Detected	
	<b>10D-Myc</b>		<b>4W-Myc</b>	
	<b>avg_logFC (SKO/WT)</b>	<b>p_adj</b>	<b>avg_logFC (SKO/WT)</b>	<b>p_adj</b>
Ccl2	0.0084754580	1.00E+00	0.0580210650	1.00E+00
Ccl4	-0.0137855930	1.00E+00	-0.0075470760	1.00E+00
Ccl5	-0.0215245270	1.00E+00	0.0672150760	1.00E+00
Ccl6	-0.0131183870	1.00E+00	0.0541973530	1.00E+00
Ccl7	Not Detected		Not Detected	
Ccl9	-0.2937460760	1.04E-01	-0.4399599750	1.99E-01
Ccl25	-0.0255756590	1.00E+00	-0.0198205990	1.00E+00
Ccl27a	0.0038820450	1.00E+00	0.1692218530	2.04E-02
Cxcl1	-0.7388919460	7.68E-24	0.0920983100	3.35E-01
Cxcl2	-0.0266341510	1.00E+00	0.0564091500	1.00E+00
Cxcl9	-0.0699571270	1.00E+00	-0.0243349200	1.00E+00
Cxcl10	-0.0341036060	1.00E+00	0.0750315600	1.00E+00
Cxcl11	-0.0073713550	1.00E+00	-0.0531037500	1.00E+00
Cxcl12	0.1090831720	6.29E-05	-0.4662282600	1.00E+00
Cxcl13	Not Detected		Not Detected	
Cxcl14	-0.0483053900	1.00E+00	0.0220272900	1.00E+00
Cxcl16	0.0247155580	1.00E+00	0.0474723400	1.00E+00
Lect2	0.2974101000	3.01E-16	0.9584413000	4.26E-66
Mif	0.4399941700	1.80E-35	0.9535501200	1.78E-80
Nampt	0.0221337400	7.23E-02	0.1122796000	6.70E-03
Spp1	0.6107580000	1.00E+00	0.6108792000	1.00E+00
Vegfa	0.0099134810	1.06E-01	0.0665659000	1.00E+00
Aimp1	Not Detected		0.1975240600	3.31E-06

**Table S4: QPCR Primer Sequences, Related to STAR Methods.**

<b>Gene</b>	<b>Forward Primer (5' - 3')</b>	<b>Reverse Primer (5' - 3')</b>
CCL2	GTTGGCTCAGCCAGATGCA	AGCCTACTCATTGGGATCATCTTG
CCL9	CCCTCTCCTTCCTCATTCTTACA	AGTCTTGAAAGCCCATGTGAAA
PD-L1	GCTCCAAAGGACTTGTACGTG	TGATCTGAAGGGCAGCATTTC
CCL17	TACCATGAGGTCACTTCAGATGC	GCACTCTCGGCCTACATTGG
CXCL10	CCTGCCACGTGTTGAGAT	TGATGGTCTTAGATTCCGGATTC
CSF1	AGTATTGCCAAGGAGGTGTCAG	TTCCTGGTCTACAAATTCAAAGG
RXR $\alpha$	CCATGAACCCTGTGAGCAG	CCTCTTGAAGAAGCCCTTGC
B-actin	TCCTGTGGCATCCACGAAACTACA	ACCAGACAGCACTGTGTTGGCATA